

# Unified description of BaBar and Belle data on the bottomonia decays

$$\Upsilon(mS) \rightarrow \Upsilon(ns)\pi^+\pi^-$$

Yurii S. Surovtsev,<sup>1</sup> Petr Bydžovský,<sup>2</sup> Thomas Gutsche,<sup>3</sup>

Robert Kamiński,<sup>4</sup> Valery E. Lyubovitskij,<sup>3,5,6</sup> and Miroslav Nagy<sup>7</sup>

<sup>1</sup>*Bogoliubov Laboratory of Theoretical Physics, Joint Institute for Nuclear Research, 141980 Dubna, Russia*

<sup>2</sup>*Nuclear Physics Institute of the AS CR, 25068 Řež, Czech Republic*

<sup>3</sup>*Institut für Theoretische Physik, Universität Tübingen,*

*Kepler Center for Astro and Particle Physics, Auf der Morgenstelle 14, D-72076 Tübingen, Germany*

<sup>4</sup>*Institute of Nuclear Physics of the PAN, Cracow 31342, Poland*

<sup>5</sup>*Department of Physics, Tomsk State University, 634050 Tomsk, Russia*

<sup>6</sup>*Mathematical Physics Department, Tomsk Polytechnic University, Lenin Avenue 30, 634050 Tomsk, Russia*

<sup>7</sup>*Institute of Physics, SAS, Bratislava 84511, Slovak Republic*

(Dated: August 11, 2021)

We present a unified analysis of the decays of bottomonia  $\Upsilon(mS) \rightarrow \Upsilon(ns)\pi\pi$  ( $m > n$ ,  $m = 2, 3, 4, 5$ ,  $n = 1, 2, 3$ ), charmonia  $J/\psi \rightarrow \phi(\pi\pi, K\bar{K})$ ,  $\psi(2S) \rightarrow J/\psi\pi\pi$ , and the isoscalar  $S$ -wave processes  $\pi\pi \rightarrow \pi\pi, K\bar{K}, \eta\eta$ . In this analysis we extend our recent study of low-lying ( $m = 2, 3$ ) radial excitations of bottomonia to modes involving higher ( $m = 4, 5$ ) excited states. Similarly as for the data on lower radial excitations, we confirm that the data for higher radially excited states from the *BABAR* and Belle collaborations can be described under conditions that the final bottomonium is a spectator and the multichannel  $\pi\pi$  scattering is considered in a model-independent approach based on analyticity, unitarity and the uniformization procedure. Indeed we show that the dipion mass distributions in the two-pion transitions of both charmonia and bottomonia states are explained by a unified mechanism based on the contribution of the  $\pi\pi$  and  $K\bar{K}$  coupled channels including their interference (final-state interactions). Therefore, our main result is that the lower and higher radially excited states of charmonia and bottomonia have no specific features in mutual comparison and can be understood in a unified picture, e.g. proposed by our approach.

PACS numbers: 11.55.Bq, 11.80.Gw, 12.39.Mk, 14.40.Pq

Keywords: coupled-channel formalism, meson-meson scattering, heavy meson decays, scalar and pseudoscalar mesons

## I. INTRODUCTION

Presently available data on bottomonia decays  $\Upsilon(mS) \rightarrow \Upsilon(ns)\pi^+\pi^-$  ( $n = 1, 2, 3$ ) extracted by different collaborations (ARGUS [1], CLEO [2], CUSB [3], Crystal Ball [4], Belle [5], and *BABAR* [6]) and for both lower and higher radial excitations of  $\Upsilon(mS)$  offer a possibility of their unified theoretical description. Recently, in Ref. [7] we focused only on the decays of lower radial excitation of bottomonia. Restriction to lower radial excitation was not specific; therefore we need to extend our analysis to higher excited states. This paper is devoted to the unified description of *BABAR* [6] and Belle [5] data on the decays  $\Upsilon(4S, 5S) \rightarrow \Upsilon(ns)\pi^+\pi^-$  ( $n = 1, 2, 3$ ) using the same set of couplings parametrizing the scattering amplitudes as in our recent study [7], where we focused on the decays of lower radial excitations of bottomonia. Now both lower and higher radial excitations of bottomonia are analyzed in a unified picture using all available data on the two-pion transitions  $\Upsilon(mS) \rightarrow \Upsilon(nS)\pi\pi$  ( $m > n$ ,  $m = 2, 3, 4, 5$ ,  $n = 1, 2, 3$ ) of the  $\Upsilon$  mesons [1]-[6]. It is important to note that the analysis of bottomonia decays has been done together with the isoscalar  $S$ -wave processes  $\pi\pi \rightarrow \pi\pi, K\bar{K}, \eta\eta$  and the charmonium decay transitions  $J/\psi \rightarrow \phi(\pi\pi, K\bar{K})$ ,  $\psi(2S) \rightarrow J/\psi\pi\pi$  using data from the Crystal Ball, DM2, Mark II, Mark III, and BES II collaborations [10]. At that, the formalism for

the analysis of multichannel  $\pi\pi$  scattering is based on analyticity, unitarity and the uniformization procedure.

One of the main objectives of our study is to shed some light on the nature of scalar mesons. The possibility for using the two-pion transitions of heavy quarkonia as a laboratory for studying the  $f_0$  mesons is related to the expectation that the dipion is produced in a relative  $S$  wave whereas the final quarkonium state remains a spectator [11]. Many efforts were undertaken to study scalar mesons, mainly by analyzing multichannel  $\pi\pi$  scattering. The problem of a unique structure interpretation of the scalar mesons is far away from being solved completely [12]. Previously we analyzed data on the decays of low-lying radial excitations of bottomonia  $\Upsilon(mS) \rightarrow \Upsilon(nS)\pi\pi$  ( $m > n$ ,  $m = 2, 3$ ,  $n = 1, 2$ ), on multichannel  $\pi\pi$  scattering, and on the charmonium decay processes. We showed [7] that the considered bottomonia decay data do not really offer new insights into the nature of the scalar mesons which were not already deduced in previous analyses of pseudoscalar-meson-scattering processes. The results of the analysis have confirmed all our earlier conclusions on the scalar mesons [10]. However, the problem must be considered further by allowing for an extended analysis including available data on the  $\Upsilon(4S, 5S)$  decays.

Note that the previous analysis of the process  $\Upsilon(3S) \rightarrow \Upsilon(1S)\pi\pi$  has already given us an opportunity to ob-

tain interesting conclusions on the mechanism of this decay [7], which is able to explain the enigmatic two-humped shape of the dipion mass distribution. This distribution might be the result of the destructive interference of the relevant contributions to the decay  $\Upsilon(3S) \rightarrow \Upsilon(1S)\pi\pi$ . However, in this scenario the phase space cuts off possible contributions, which might interfere destructively with the  $\pi\pi$ -scattering contribution giving the specific shape of the dipion spectrum. In a number of works (see, e.g., Ref. [13] and the references therein, and our discussion in Ref. [7]) various (sometimes rather doubtful) assumptions were made to obtain the needed result. We have explained this effect on the basis of our previous conclusions without any additional assumptions. In Refs. [10, 14, 15] we have shown the following: if a wide resonance cannot decay into a channel which opens above its mass, and if the resonance is strongly coupled to this channel [e.g.  $f_0(500)$  and the  $K\bar{K}$  channel], then this resonance should be treated as a multichannel state. The closed channel should be included while taking into account the Riemann-surface sheets related to the threshold branch point of this channel and performing the combined analysis of the coupled channels.

In the present extension we include the  $\Upsilon(4S)$  and  $\Upsilon(5S)$  which are distinguished from the lower  $\Upsilon$  states by the fact that their masses are above the  $B\bar{B}$  thresholds. These higher states predominantly decay into pairs of the  $B$ -meson family because these modes are not suppressed by the OZI rule: the  $\Upsilon(4S)$  decays into  $B\bar{B}$  pairs form more than 96% of the total width; for the  $\Upsilon(5S)$  these decay modes make up about 90%. Therefore, there naturally appears a desire to use this fact in explaining the characteristic shape of the dipion mass distribution in the decays  $\Upsilon(mS) \rightarrow \Upsilon(nS)\pi\pi$  ( $m > n$ ,  $m = 2, 3, 4, 5$ ,  $n = 1, 2, 3$ ). E.g., in Ref. [16], one supposed that a pion pair is formed in the  $\Upsilon(4S)$  decay both as a direct production and as the sequential process  $\Upsilon(4S) \rightarrow B\bar{B} \rightarrow \Upsilon(nS) + f_0 \rightarrow \Upsilon(nS) + \pi^+\pi^-$  ( $n = 1, 2$ ). Though an allowance for contributions of these two mechanisms with a relative phase reproduces satisfactorily the data on decays  $\Upsilon(4S) \rightarrow \Upsilon(2S, 1S)\pi^+\pi^-$ , it seems that the former assumption is not reasonable because the pions interact strongly.

In contrast to the very big contributions to the total widths of the  $\Upsilon(4S, 5S)$  from decays into pairs of the  $B$ -meson family, the processes of interest are strongly reduced decay modes: the decays  $\Upsilon(4S) \rightarrow \Upsilon(1S)\pi\pi$  and  $\Upsilon(4S) \rightarrow \Upsilon(2S)\pi\pi$  form about  $(8.1 \pm 0.6) \times 10^{-5}\%$  and  $(8.6 \pm 1.3) \times 10^{-5}\%$  of the total width, and  $\Upsilon(5S) \rightarrow \Upsilon(1S, 2S, 3S)\pi\pi$ ,  $(5 \div 8) \times 10^{-3}\%$  [12]. The total widths of  $\Upsilon(5S)$  and  $\Upsilon(4S)$  are 110 and 20.5 MeV, respectively, and the one of the  $\Upsilon(3S)$  (on which we already have clarified the mechanism of the two-pion transitions [7]) is 20.32 keV. The partial decay widths of  $\Upsilon(5S) \rightarrow \Upsilon(1S, 2S, 3S)\pi\pi$  are almost of the same order as the ones of the decays  $\Upsilon(3S) \rightarrow \Upsilon(1S, 2S)\pi\pi$ . The decay widths of  $\Upsilon(4S) \rightarrow \Upsilon(1S, 2S)\pi\pi$  are even smaller than the latter ones by about 2 orders of magnitude.

The above comparison of decay widths implies that in the two-pion transitions of  $\Upsilon(4S)$  and  $\Upsilon(5S)$  the basic mechanism, which explains the dipion mass distributions, cannot be related to the  $B\bar{B}$  transition dynamics. We shall show that the two-pion transitions both of bottomonia and charmonia are explained by a unified mechanism. It is based on our previous conclusions on the wide resonances [10, 14, 15] and is related to the interference of the contributions of multichannel  $\pi\pi$  scattering in the final-state interaction.

We also work out the role of the individual  $f_0$  resonances in contributing to the dipion mass distributions in the decays  $\Upsilon(4S, 5S) \rightarrow \Upsilon(nS)\pi^+\pi^-$  ( $n = 1, 2, 3$ ). For this purpose, in the Appendix, we summarize and discuss some formulas and results from our previous paper [10].

## II. MULTICHANNEL $\pi\pi$ SCATTERING IN TWO-PION TRANSITIONS OF BOTTOMONIA

When carrying out our analysis, data for the processes  $\pi\pi \rightarrow \pi\pi, K\bar{K}, \eta\eta$  are taken from many sources (see the corresponding references in [10]). Formalism for analyzing the multichannel  $\pi\pi$  scattering is presented briefly in the Appendix. The combined analysis including decay data on  $J/\psi \rightarrow \phi(\pi\pi, K\bar{K})$  and  $\psi(2S) \rightarrow J/\psi\pi\pi$  from the Mark III, DM2, BES II, Mark II, and Crystal Ball collaborations (see corresponding references also in [10]) was found to be important for getting unique solutions to the  $f_0$ -meson parameters: first we solved the ambiguity in the parameters of the  $f_0(500)$  [17] in favor of the wider state; second, the parameters of the other  $f_0$  mesons had small corrections [10]. A further addition of decay data on  $\Upsilon(mS) \rightarrow \Upsilon(nS)\pi\pi$  ( $m > n$ ,  $m = 2, 3$ ,  $n = 1, 2$ ) from ARGUS, CLEO, CUSB, and the Crystal Ball collaborations in a combined analysis did not add any new constraints on the  $f_0$  mesons, thus confirming the previous conclusions about these states. However, the analysis resulted in an interesting explanation of the enigmatic two-humped shape of the dipion spectrum in the decay  $\Upsilon(3S) \rightarrow \Upsilon(1S)\pi\pi$ : this shape is proved to be stipulated by a destructive interference of the  $\pi\pi$  and  $K\bar{K}$  coupled-channel contributions to the final state of this decay [7].

In the present manuscript we further extend the analysis of the two-pion transitions of radially excited  $\Upsilon$  mesons to higher states —  $\Upsilon(4S)$  and  $\Upsilon(5S)$ . The used formalism for calculating the dimeson mass distributions in the  $\Upsilon(mS)$  decays is analogous to the one proposed in Ref. [11] for the decays  $J/\psi \rightarrow \phi(\pi\pi, K\bar{K})$  and  $V' \rightarrow V\pi\pi$  ( $V = \psi, \Upsilon$ ). I.e., it was assumed that the pion pairs in the final state have zero isospin and spin. Only these pairs of pions undergo final-state interactions whereas the final  $\Upsilon(nS)$  meson ( $n < m$ ) acts as a spectator. This decay model is justified by the consideration of quark diagrams for the processes of interest and by allowance for the fact that we deal with the two-pion transitions of the radially excited states to lower ones of the same family; therefore, it is reasonable to ex-

pect that the dipion is produced in a relative  $S$  wave and the final bottomonium state remains the spectator. The amplitudes for the decays  $\Upsilon(mS) \rightarrow \Upsilon(nS)\pi\pi$  ( $m > n$ ,  $m = 2, 3, 4, 5$ ,  $n = 1, 2, 3$ ) include the scattering amplitudes  $T_{ij}$  ( $i, j = 1 - \pi\pi, 2 - K\bar{K}$ ) as follows:

$$F_{mn}(s) = (\rho_{mn}^0 + \rho_{mn}^1 s) T_{11} + (\omega_{mn}^0 + \omega_{mn}^1 s) T_{21}, \quad (1)$$

where indices  $m$  and  $n$  correspond to  $\Upsilon(mS)$  and  $\Upsilon(nS)$ , respectively. The free parameters  $\rho_{mn}^0$ ,  $\rho_{mn}^1$ ,  $\omega_{mn}^0$ , and  $\omega_{mn}^1$  depend on the couplings of the  $\Upsilon(mS)$  to the channels  $\pi\pi$  and  $K\bar{K}$ . The model-independent amplitudes  $T_{ij}$  are expressed through the  $S$ -matrix elements shown in the Appendix

$$S_{ij} = \delta_{ij} + 2i\sqrt{\rho_1\rho_2} T_{ij}, \quad (2)$$

where  $\rho_i = \sqrt{1 - s_i/s}$  and  $s_i$  is the reaction threshold. The expressions for the dipion mass distributions in the decay  $\Upsilon(mS) \rightarrow \Upsilon(nS)\pi\pi$  are

$$N|F|^2 \sqrt{(s - s_1)\lambda(m_{\Upsilon(mS)}^2, s, m_{\Upsilon(nS)}^2)}, \quad (3)$$

where  $\lambda(x, y, z) = x^2 + y^2 + z^2 - 2xy - 2yz - 2xz$  is the Källén function. The normalization constants  $N$  are determined by a fit to the specific experiment and collected in Table I. Parameters of the coupling functions of the decay particles  $\Upsilon(mS)$  ( $m = 2, \dots, 5$ ) to channel  $i$  obtained in the analysis are shown in Tables II and III. A satisfactory combined description of all considered processes is obtained with a total  $\chi^2/\text{ndf} = 824.236/(714 - 91) \approx 1.32$ . The  $\chi^2/\text{ndp}$  (ndp is number of data points) estimates for the processes  $\pi\pi \rightarrow \pi\pi, K\bar{K}, \eta\eta$ , and specific decay modes are collected in Table IV.

In Figs. 1 and 2 we show the fits (solid lines) to the experimental data of the *BABAR* [6] and Belle [5] collaborations on the bottomonia decays —  $\Upsilon(4S, 5S) \rightarrow \Upsilon(nS)\pi^+\pi^-$  ( $n = 1, 2, 3$ ) — in the combined analysis with the lower bottomonia decays —  $\Upsilon(mS) \rightarrow \Upsilon(nS)\pi\pi$  ( $m > n, m = 2, 3, n = 1, 2$ ) — with the processes  $\pi\pi \rightarrow \pi\pi, K\bar{K}, \eta\eta$ , and the charmonia decays —  $J/\psi \rightarrow \phi(\pi\pi, K\bar{K}), \psi(2S) \rightarrow J/\psi\pi\pi$ . The curves demonstrate an interesting behavior — a bell-shaped form in the near- $\pi\pi$ -threshold region [especially for the  $\Upsilon(4S) \rightarrow \Upsilon(2S)\pi^+\pi^-$ ], smooth dips near a dipion mass of 0.6 GeV in  $\Upsilon(4S, 5S) \rightarrow \Upsilon(1S)\pi^+\pi^-$  and of about 0.44 GeV in  $\Upsilon(4S) \rightarrow \Upsilon(2S)\pi^+\pi^-$ , and sharp dips of about 1 GeV in the  $\Upsilon(4S, 5S) \rightarrow \Upsilon(1S)\pi^+\pi^-$  transition. This shape of the dipion mass distribution is obviously explained by the interference between the  $\pi\pi$ -scattering and  $K\bar{K} \rightarrow \pi\pi$  contributions to the final states of these decays — by the constructive interference in the near- $\pi\pi$ -threshold region and by a destructive one in the dip regions. Whereas the data on  $\Upsilon(5S) \rightarrow \Upsilon(1S)\pi^+\pi^-$  confirm the sharp dips

TABLE I: Normalization constants  $N$ .

Process	$N$	Collaboration
$\Upsilon(2S) \rightarrow \Upsilon(1S)\pi^+\pi^-$	4.3439	ARGUS [1]
$\Upsilon(2S) \rightarrow \Upsilon(1S)\pi^+\pi^-$	2.1776	CLEO [2]
$\Upsilon(2S) \rightarrow \Upsilon(1S)\pi^+\pi^-$	1.2011	CUSB [3]
$\Upsilon(2S) \rightarrow \Upsilon(1S)\pi^0\pi^0$	0.0788	Crystal Ball [4]
$\Upsilon(3S) \rightarrow \Upsilon(1S)\pi^+\pi^-$	0.5096	CLEO [8]
$\Upsilon(3S) \rightarrow \Upsilon(1S)\pi^0\pi^0$	0.2235	CLEO [8]
$\Upsilon(3S) \rightarrow \Upsilon(2S)\pi^+\pi^-$	7.7397	CLEO [9]
$\Upsilon(3S) \rightarrow \Upsilon(2S)\pi^0\pi^0$	3.8587	CLEO [9]
$\Upsilon(4S) \rightarrow \Upsilon(1S)\pi^+\pi^-$	7.1476	<i>BABAR</i> [6]
$\Upsilon(4S) \rightarrow \Upsilon(1S)\pi^+\pi^-$	0.5553	Belle [5]
$\Upsilon(4S) \rightarrow \Upsilon(2S)\pi^+\pi^-$	58.143	<i>BABAR</i> [6]
$\Upsilon(5S) \rightarrow \Upsilon(1S)\pi^+\pi^-$	0.1626	Belle [5]
$\Upsilon(5S) \rightarrow \Upsilon(2S)\pi^+\pi^-$	4.8355	Belle [5]
$\Upsilon(5S) \rightarrow \Upsilon(3S)\pi^+\pi^-$	10.858	Belle [5]

TABLE II: Parameters of the coupling functions  $\rho_{ij}^k$ .

Parameter	Numerical value	Parameter	Numerical value
$\rho_{21}^0$	0.4050	$\rho_{21}^1$	47.0963
$\rho_{31}^0$	1.0827	$\rho_{31}^1$	-2.7546
$\rho_{32}^0$	7.3875	$\rho_{32}^1$	-2.5598
$\rho_{41}^0$	0.6162	$\rho_{41}^1$	-2.5715
$\rho_{42}^0$	2.3290	$\rho_{42}^1$	-7.3511
$\rho_{51}^0$	0.7078	$\rho_{51}^1$	4.0132
$\rho_{52}^0$	0.8133	$\rho_{52}^1$	2.2061
$\rho_{53}^0$	0.8946	$\rho_{53}^1$	2.5380

TABLE III: Parameters of the coupling functions  $\omega_{ij}^k$ .

Parameter	Numerical value	Parameter	Numerical value
$\omega_{21}^0$	1.3352	$\omega_{21}^1$	-21.4343
$\omega_{31}^0$	0.8615	$\omega_{31}^1$	0.6600
$\omega_{32}^0$	0.0	$\omega_{31}^1$	0.0
$\omega_{41}^0$	-0.8467	$\omega_{41}^1$	0.2128
$\omega_{42}^0$	1.8096	$\omega_{42}^1$	-10.1477
$\omega_{51}^0$	4.8380	$\omega_{51}^1$	-3.9091
$\omega_{52}^0$	-0.7973	$\omega_{52}^1$	0.3247
$\omega_{53}^0$	0.6270	$\omega_{51}^1$	-0.0483

TABLE IV:  $\chi^2/\text{ndp}$  estimates for specific decay modes.

Process	$\chi^2/\text{ndp}$
$\pi\pi$ scattering	0.90
$\pi\pi \rightarrow K\bar{K}$	1.16
$\pi\pi \rightarrow \eta\eta$	0.87
$J/\psi \rightarrow \phi(\pi^+\pi^-, K^+K^-)$	1.36
$\psi(2S) \rightarrow J/\psi(\pi^+\pi^-, \pi^0\pi^0)$	2.43
$\Upsilon(2S) \rightarrow \Upsilon(1S)(\pi^+\pi^-, \pi^0\pi^0)$	1.01
$\Upsilon(3S) \rightarrow \Upsilon(1S)(\pi^+\pi^-, \pi^0\pi^0)$	0.67
$\Upsilon(3S) \rightarrow \Upsilon(2S)(\pi^+\pi^-, \pi^0\pi^0)$	0.61
$\Upsilon(4S) \rightarrow \Upsilon(1S)(\pi^+\pi^-)$	0.27
$\Upsilon(4S) \rightarrow \Upsilon(2S)(\pi^+\pi^-)$	0.27
$\Upsilon(5S) \rightarrow \Upsilon(1S)(\pi^+\pi^-)$	1.80
$\Upsilon(5S) \rightarrow \Upsilon(2S)(\pi^+\pi^-)$	1.08
$\Upsilon(5S) \rightarrow \Upsilon(3S)(\pi^+\pi^-)$	0.81

TABLE V: Background parameters for the minimal set of scalar mesons  $f_0(500)$ ,  $f_0(980)$  and  $f'_0(1500)$ .

$a_{11}$	$a_{1\sigma}$	$a_{1v}$
0.0	0.0321	0.0
$b_{11}$	$b_{1\sigma}$	$b_{1v}$
-0.0051	0.0	0.04
$a_{21}$	$a_{2\sigma}$	$a_{2v}$
-1.6425	-0.3907	-7.274
$b_{21}$	$b_{2\sigma}$	$b_{2v}$
0.1189	0.2741	5.823
$b_{31}$	$b_{3\sigma}$	$b_{3v}$
0.7711	0.505	0.0

TABLE VI: Background parameters for the set of scalar mesons when the  $f_0(500)$  is switched off.

$a_{11}$	$a_{1\sigma}$	$a_{1v}$
0.3513	-0.2055	0.207
$b_{11}$	$b_{1\sigma}$	$b_{1v}$
-0.0077	0.0	0.0378
$a_{21}$	$a_{2\sigma}$	$a_{2v}$
-1.8597	0.1688	-7.519
$b_{21}$	$b_{2\sigma}$	$b_{2v}$
0.161	0.0	6.94
$b_{31}$	$b_{3\sigma}$	$b_{3v}$
0.7758	0.4985	0.0

near 1 GeV, the scarce data on  $\Upsilon(4S) \rightarrow \Upsilon(1S)\pi^+\pi^-$  do not allow for such a unique conclusion yet. We further investigated the role of the individual  $f_0$  resonances in contributing to the shape of the dipion mass distributions in the decays  $\Upsilon(4S, 5S) \rightarrow \Upsilon(nS)\pi^+\pi^-$  ( $n = 1, 2, 3$ ). In this case we switched off only those resonances [ $f_0(500)$ ,  $f_0(1370)$ ,  $f_0(1500)$  and  $f_0(1710)$ ], removal of which can be somehow compensated by correcting the background (maybe, with elements of the pseudobackground) to have the more-or-less acceptable description of the multichannel  $\pi\pi$  scattering.

First, when leaving out before-mentioned resonances, a minimal set of the  $f_0$  mesons consisting of the  $f_0(500)$ ,  $f_0(980)$ , and  $f'_0(1500)$  is sufficient to achieve a description of the processes  $\pi\pi \rightarrow \pi\pi, K\bar{K}, \eta\eta$  with a total  $\chi^2/\text{ndf} \approx 1.20$ . The obtained, adjusted background parameters are shown in Table V.

Second, from these three mesons only the  $f_0(500)$  can be switched off while still obtaining a reasonable description of multichannel  $\pi\pi$  scattering (though with an appearance of the pseudobackground) with a total  $\chi^2/\text{ndf} \approx 1.43$  and with the corrected background parameters, which are shown in Table VI.

In Figs. 1 and 2 variants of the calculations of the dipion mass distributions with contributions from the  $f_0(500)$ ,  $f_0(980)$ , and  $f'_0(1500)$  and from the  $f_0(980)$ , and  $f'_0(1500)$  are shown by the dotted and dashed lines, respectively. It is seen that the sharp dips near 1 GeV in the  $\Upsilon(4S, 5S)$  decays are related to the  $f_0(500)$  contribution in the interfering amplitudes of  $\pi\pi$  scattering and the  $K\bar{K} \rightarrow \pi\pi$  process.

One should also note the unexpected result — a considerable contribution of the  $f_0(1370)$  to the bell-shaped form in the near- $\pi\pi$ -threshold region, especially in the decay  $\Upsilon(4S) \rightarrow \Upsilon(2S)\pi\pi$ . This is interesting because the  $f_0(1370)$  is predominantly the  $s\bar{s}$  state according to the earlier analysis [10] and practically does not contribute to the  $\pi\pi$ -scattering amplitude. However, this state influences noticeably the  $K\bar{K}$  scattering; e.g., it was shown that the  $K\bar{K}$ -scattering length is very sensitive to whether this state exists or not [18].

### III. SUMMARY

We performed a combined analysis of data on isoscalar  $S$ -wave processes  $\pi\pi \rightarrow \pi\pi, K\bar{K}, \eta\eta$ , on the decays of the charmonia —  $J/\psi \rightarrow \phi(\pi\pi, K\bar{K}), \psi(2S) \rightarrow J/\psi\pi\pi$  — and of the bottomonia —  $\Upsilon(mS) \rightarrow \Upsilon(nS)\pi\pi$  ( $m > n$ ,  $m = 2, 3, 4, 5$ ,  $n = 1, 2, 3$ ) from the ARGUS, Crystal Ball, CLEO, CUSB, DM2, Mark II, Mark III, BES II, *BABAR*, and Belle collaborations. It is interesting that the expansion of the analyzed data by adding the ones on the above bottomonia decays does not change practically the values of the fitted resonance and background parameters in comparison with the combined analysis only of the above multichannel  $\pi\pi$  scattering and charmonia decays. Therefore, it is possible and reasonable to consider that

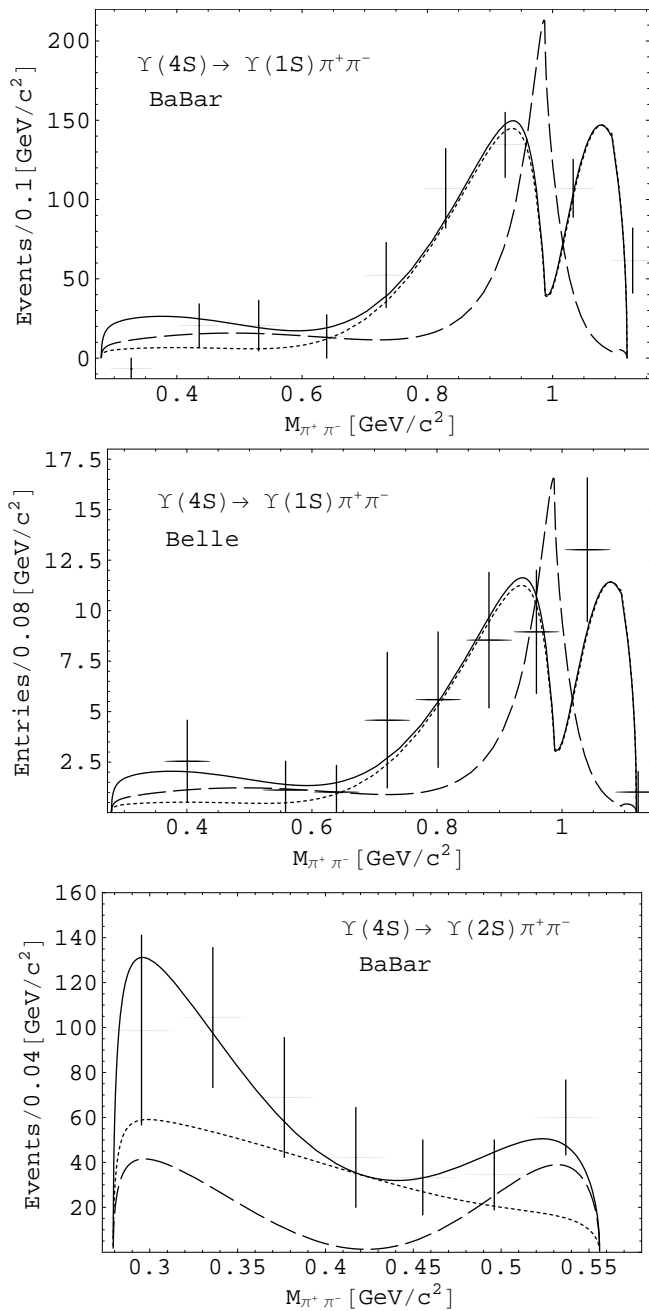


FIG. 1: The decays  $\Upsilon(4S) \rightarrow \Upsilon(1S)\pi\pi$  and  $\Upsilon(4S) \rightarrow \Upsilon(2S)\pi\pi$ . The solid lines correspond to the contribution of all relevant resonances; the dotted, of the  $f_0(500)$ ,  $f_0(980)$ , and  $f'_0(1500)$ ; the dashed, of the  $f_0(980)$  and  $f'_0(1500)$ .

these parameters are fixed by the latter.

Here we specifically focused on the unified description of *BABAR* [6] and Belle [5] data on the decays  $\Upsilon(4S,5S) \rightarrow \Upsilon(nS)\pi^+\pi^-$  ( $n = 1, 2, 3$ ). It was shown that the dipion mass distributions in the two-pion transitions both of charmonia and bottomonia are explained by a unified mechanism related to contributions of the  $\pi\pi$  and  $K\bar{K}$  coupled channels and their interference. The

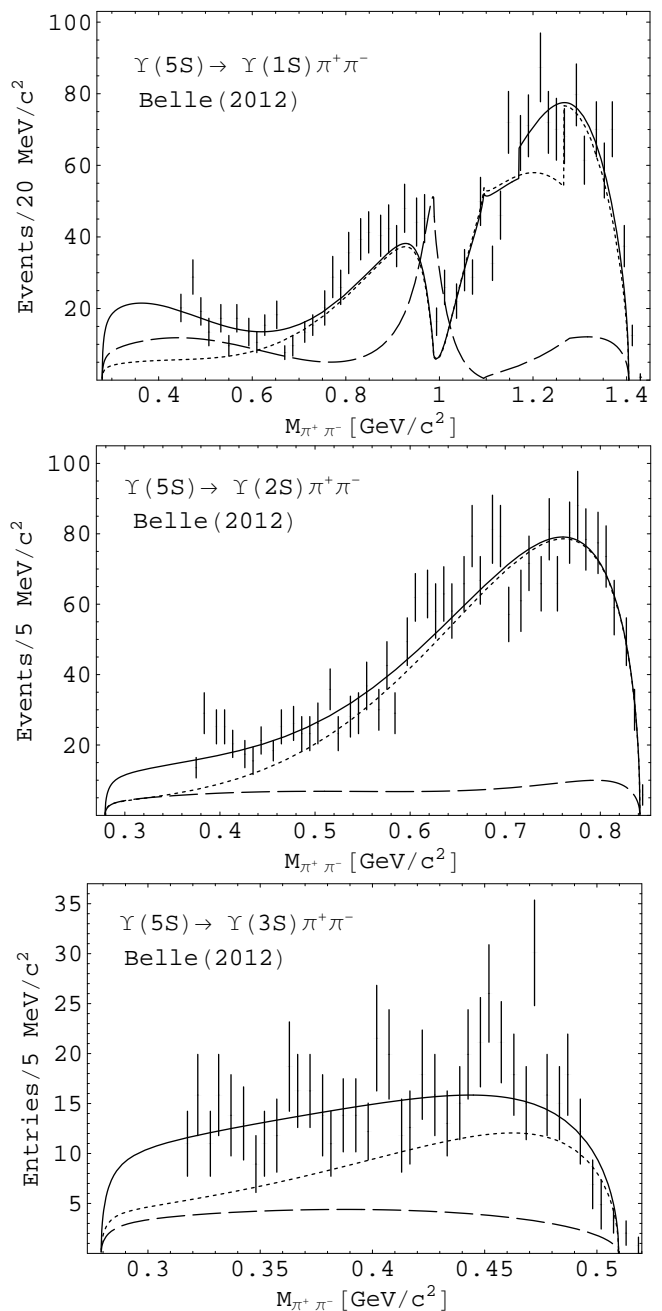


FIG. 2: The decays  $\Upsilon(5S) \rightarrow \Upsilon(nS)\pi^+\pi^-$  ( $n = 1, 2, 3$ ). The solid lines correspond to the contribution of all relevant resonances; the dotted, of the  $f_0(500)$ ,  $f_0(980)$ , and  $f'_0(1500)$ ; the dashed, of the  $f_0(980)$  and  $f'_0(1500)$ .

role of the individual  $f_0$  resonances in making up the shape of the dipion mass distributions in these decays was considered.

When describing the bottomonia decays, we did not change the resonance parameters in comparison with the ones obtained in the combined analysis of the processes  $\pi\pi \rightarrow \pi\pi, K\bar{K}, \eta\eta$ , and charmonia decays [10, 19]. Thus,

the results of the analysis confirmed all of our earlier conclusions on the scalar mesons [10].

### Acknowledgments

This work was supported in part by the Heisenberg-Landau Program, the Votruba-Blokhintsev Program for Cooperation of Czech Republic with JINR, the Grant Agency of the Czech Republic (Grant No. P203/15/04301), the Grant Program of Plenipotentiary of Slovak Republic at JINR, the Bogoliubov-Infeld Program for Cooperation of Poland with JINR, the Tomsk State University Competitiveness Improvement Program, the Russian Federation program ‘‘Nauka’’ (Contract No. 0.1526.2015, 3854), Slovak Grant Agency VEGA under Contract No. 2/0197/14, and by the Polish National Science Center (NCN) Grant No. DEC-2013/09/B/ST2/04382.

### Appendix A: The model-independent amplitudes for multi-channel $\pi\pi$ scattering

Considering multichannel  $\pi\pi$  scattering, we shall deal with the three-channel case (namely with  $\pi\pi \rightarrow \pi\pi, K\bar{K}, \eta\eta$ ) because it was shown [14, 15] that this is a minimal number of coupled channels needed for obtaining reasonable and correct values of the scalar-isoscalar resonance parameters.

The three-channel  $S$  matrix is determined on the eight-sheeted Riemann surface. The matrix elements  $S_{ij}$ , where  $i, j = 1, 2, 3$  denote the channels, have right-hand cuts along the real axis of the complex  $s$  plane ( $s$  is the invariant total energy squared); starting with the channel thresholds  $s_i$  ( $i = 1, 2, 3$ ), the left-hand cuts are related to the crossed channels. The Riemann-surface sheets are numbered according to the signs of the analytic continuations of the quantities  $\sqrt{s - s_i}$  as follows:  $\text{signs}(\text{Im}\sqrt{s - s_1}, \text{Im}\sqrt{s - s_2}, \text{Im}\sqrt{s - s_3}) = +++, -++, --+, +-+, +--, ----, -+--, ++-$  correspond to sheets I, II,  $\dots$ , VIII, respectively.

The Riemann-surface structure can be represented by taking the following uniformizing variable [17] where we have neglected the  $\pi\pi$ -threshold branch point and included the  $K\bar{K}$ - and  $\eta\eta$ -threshold branch points and the left-hand branch point at  $s = 0$  related to the crossed channels with

$$w = \frac{\sqrt{(s - s_2)s_3} + \sqrt{(s - s_3)s_2}}{\sqrt{s(s_3 - s_2)}}, \quad (\text{A1})$$

where  $s_2 = 4m_K^2$  and  $s_3 = 4m_\eta^2$ . Resonance representations on the Riemann surface are obtained using formulas from [17]. Analytic continuations of the  $S$ -matrix elements to all sheets are expressed in terms of those on the physical (I) sheet that have only the resonance zeros

(beyond the real axis), at least around the physical region. Then multichannel resonances are classified. For analytic continuations the resonance poles on sheets II, IV, and VIII, which are not shifted due to the coupling of channels, correspond to zeros on the physical sheet in  $S_{11}$ ,  $S_{22}$  and  $S_{33}$ , respectively. They are at the same points on the energy plane as the resonance poles (for more details see Ref. [17]). It is convenient to classify multichannel resonances according to resonance zeros on sheet I. In the three-channel case there are *seven types* of resonances corresponding to seven possible situations when there are resonance zeros on sheet I only in  $S_{11}$  – (a),  $S_{22}$  – (b),  $S_{33}$  – (c),  $S_{11}$  and  $S_{22}$  – (d),  $S_{22}$  and  $S_{33}$  – (e),  $S_{11}$  and  $S_{33}$  – (f),  $S_{11}$ ,  $S_{22}$ , and  $S_{33}$  – (g). The resonance of every type is represented by a pair of complex-conjugate *clusters* (of poles and zeros on the Riemann surface).

The  $S$ -matrix elements  $S_{ij}$  are parametrized using the Le Couteur–Newton relations [20]. They express the  $S$ -matrix elements of all coupled processes in terms of the Jost determinant  $d(\sqrt{s - s_1}, \dots, \sqrt{s - s_n})$  which is a real analytic function with the only square-root branch points at  $\sqrt{s - s_i} = 0$ . On the  $w$  plane, the Le Couteur–Newton relations are [17]

$$S_{11} = \frac{d^*(-w^*)}{d(w)}, \quad S_{22} = \frac{d(-w^{-1})}{d(w)}, \quad S_{33} = \frac{d(w^{-1})}{d(w)}, \quad (\text{A2})$$

$$S_{11}S_{22} - S_{12}^2 = \frac{d^*(w^{*-1})}{d(w)}, \quad S_{11}S_{33} - S_{13}^2 = \frac{d^*(-w^{*-1})}{d(w)}$$

where now  $d(w)$  is free from any branch points. The  $S$ -matrix elements are taken as the products  $S = S_B S_{res}$ ; the main (*model-independent*) contribution of resonances given by the pole clusters is included in the resonance part  $S_{res}$ ; possible remaining small (*model-dependent*) contributions of resonances and the influence of channels which are not taken explicitly into account in the uniformizing variable are included in the background part  $S_B$ . The  $d_{res}(w)$  function for the resonance part, which now is free from any branch points, is taken as

$$d_{res}(w) = w^{-\frac{M}{2}} \prod_{r=1}^M (w + w_r^*), \quad (\text{A3})$$

where  $M$  is the number of resonance zeros. For the background part we have

$$d_B = \exp\left[-i \sum_{n=1}^3 \frac{\sqrt{s - s_n}}{2m_n} (\alpha_n + i\beta_n)\right] \quad (\text{A4})$$

with

$$\alpha_n = a_{n1} + a_{n\sigma} \frac{s - s_\sigma}{s_\sigma} \theta(s - s_\sigma) + a_{nv} \frac{s - s_v}{s_v} \theta(s - s_v),$$

$$\beta_n = b_{n1} + b_{n\sigma} \frac{s - s_\sigma}{s_\sigma} \theta(s - s_\sigma) + b_{nv} \frac{s - s_v}{s_v} \theta(s - s_v)$$

where  $s_\sigma$  is the  $\sigma\sigma$  threshold,  $s_v$  the combined threshold of the  $\eta\eta'$ ,  $\rho\rho$ ,  $\omega\omega$  channels, which were obtained

in the analysis. The resonance zeros  $w_r$  and the background parameters were fixed by fitting to the data on  $\pi\pi \rightarrow \pi\pi, K\bar{K}, \eta\eta$ , and the charmonium decay processes —  $J/\psi \rightarrow \phi(\pi\pi, K\bar{K}), \psi(2S) \rightarrow J/\psi\pi\pi$  [10].

The preferred scenario found is when the  $f_0(500)$  is de-

scribed by the cluster of type **(a)**, the  $f_0(1370)$ ,  $f_0(1500)$ , and  $f_0(1710)$  with type **(c)**, and  $f'_0(1500)$  by type **(g)**; the  $f_0(980)$  is represented only by the pole on sheet II and a shifted pole on sheet III. The obtained pole clusters for the resonances are shown in Table VII.

TABLE VII: The pole clusters for resonances in the  $\sqrt{s}$  plane. The poles corresponding to the  $f'_0(1500)$  on sheets III, V and VII are of second order and that on sheet VI of third order in our approximation.  $\sqrt{s_r} = E_r - i\Gamma_r/2$ .

Sheet		$f_0(500)$	$f_0(980)$	$f_0(1370)$	$f_0(1500)$	$f'_0(1500)$	$f_0(1710)$
II	$E_r$	$514.5 \pm 12.4$	$1008.1 \pm 3.1$			$1512.7 \pm 4.9$	
	$\Gamma_r/2$	$465.6 \pm 5.9$	$32.0 \pm 1.5$			$285.8 \pm 12.9$	
III	$E_r$	$544.8 \pm 17.7$	$976.2 \pm 5.8$	$1387.6 \pm 24.4$		$1506.2 \pm 9.0$	
	$\Gamma_r/2$	$465.6 \pm 5.9$	$53.0 \pm 2.6$	$166.9 \pm 41.8$		$127.9 \pm 10.6$	
IV	$E_r$			$1387.6 \pm 24.4$		$1512.7 \pm 4.9$	i
	$\Gamma_r/2$			$178.5 \pm 37.2$		$216.0 \pm 17.6$	
V	$E_r$			$1387.6 \pm 24.4$	$1493.9 \pm 3.1$	$1498.9 \pm 7.2$	$1732.8 \pm 43.2$
	$\Gamma_r/2$			$260.9 \pm 73.7$	$72.8 \pm 3.9$	$142.2 \pm 6.0$	$114.8 \pm 61.5$
VI	$E_r$	$566.5 \pm 29.1$		$1387.6 \pm 24.4$	$1493.9 \pm 5.6$	$1511.4 \pm 4.3$	$1732.8 \pm 43.2$
	$\Gamma_r/2$	$465.6 \pm 5.9$		$249.3 \pm 83.1$	$58.4 \pm 2.8$	$179.1 \pm 4.0$	$111.2 \pm 8.8$
VII	$E_r$	$536.2 \pm 25.5$			$1493.9 \pm 5.0$	$1500.5 \pm 9.3$	$1732.8 \pm 43.2$
	$\Gamma_r/2$	$465.6 \pm 5.9$			$47.8 \pm 9.3$	$99.7 \pm 18.0$	$55.2 \pm 38.0$
VIII	$E_r$				$1493.9 \pm 3.2$	$1512.7 \pm 4.9$	$1732.8 \pm 43.2$
	$\Gamma_r/2$				$62.2 \pm 9.2$	$299.6 \pm 14.5$	$58.8 \pm 16.4$

The obtained background parameters are shown in Table VIII.

The small (zero for the elastic region) values of the  $\pi\pi$ -scattering background parameters (obtained after allowing for the left-hand branch point at  $s = 0$ ) confirms our assumption  $S = S_B S_{res}$  and also that the representation of multichannel resonances by the pole clusters on the uniformization plane is good and quite sufficient.

It is important that we have practically obtained zero background for  $\pi\pi$  scattering in the scalar-isoscalar channel because a reasonable and simple description of the background should be a criterion for the correctness of the approach. This shows that the consideration of the left-hand branch point at  $s = 0$  in the uniformizing variable partly solves a problem of some approaches (see, e.g., Ref. [21]) where the wide-resonance parameters are strongly controlled by the nonresonant background.

Another important conclusion in our approach is also related to a practically zero background in  $\pi\pi$ -scattering: the contribution to the  $\pi\pi$  scattering amplitude from the crossed channels is given by allowing for the left-hand branch point at  $s = 0$  in the uniformizing variable and the meson-exchange contributions in the left-

hand cuts. The zero background in the elastic-scattering region is obtained only when taking into account the left-hand branch point in the proper uniformizing variables both in the two-channel analysis of the processes  $\pi\pi \rightarrow \pi\pi, K\bar{K}$  [18] and in the three-channel analysis of the processes  $\pi\pi \rightarrow \pi\pi, K\bar{K}, \eta\eta$ . This indicates that the  $\rho$ - and  $f_0(500)$ -meson-exchange contributions in the left-hand cut practically cancel each other. One can show allowing for gauge invariance that the vector- and scalar-meson exchanges contribute with opposite signs. Therefore, the practically zero background in  $\pi\pi$  scattering is an additional confirmation that the  $f_0(500)$  observed in the analysis as the pole cluster of type **a** is indeed a particle (though very wide), not some dynamically formed resonance. Therefore, one must consider at least in the background the coupled  $\sigma\sigma$  channel which is not taken into account explicitly in the uniformizing variable (A1). In this connection it is reasonable to interpret the effective threshold at  $s_\sigma = 1.6338 \text{ GeV}^2$  in the background phase shift of the  $\pi\pi$ -scattering amplitude as related to the  $\sigma\sigma$  channel. Only in this channel we have obtained a nonzero background phase shift in  $\pi\pi$  scattering ( $a_{1\sigma} = 0.0199$ ).

TABLE VIII: Background parameters for the preferred scenario.

$a_{11}$	$a_{1\sigma}$	$a_{1v}$
0.0	0.0199	0.0
$b_{11}$	$b_{1\sigma}$	$b_{1v}$
0.0	0.0	0.0338
$a_{21}$	$a_{2\sigma}$	$a_{2v}$
-2.4649	-2.3222	-6.611
$b_{21}$	$b_{2\sigma}$	$b_{2v}$
0.0	0.0	7.073
$b_{31}$	$b_{3\sigma}$	$b_{3v}$
0.6421	0.4851	0.0
$s_\sigma$	$s_v$	
1.6338 GeV <sup>2</sup>	2.0857 GeV <sup>2</sup>	

- [1] H. Albrecht *et al.* (ARGUS Collaboration), Phys. Lett. **134B**, 137 (1984).
- [2] D. Besson *et al.* (CLEO Collaboration), Phys. Rev. D **30**, 1433 (1984).
- [3] V. Fonseca *et al.* (CUSB Collaboration), Nucl. Phys. **B242**, 31 (1984).
- [4] D. Gelfman *et al.* (Crystal Ball Collaboration), Phys. Rev. D **32**, 2893 (1985).
- [5] A. Sokolov *et al.* (Belle Collaboration), Phys. Rev. D **75**, 071103 (2007); A. Bondar *et al.* (Belle Collaboration), Phys. Rev. Lett. **108**, 122001 (2012).
- [6] B. Aubert *et al.* (BABAR Collaboration), Phys. Rev. Lett. **96**, 232001 (2006).
- [7] Yu. S. Surovtsev, P. Bydžovský, T. Gutsche, R. Kamiński, V. E. Lyubovitskij, and M. Nagy, Phys. Rev. D **91**, 037901 (2015).
- [8] D. Cronin-Hennessy *et al.* (CLEO Collaboration), Phys. Rev. D **76**, 072001 (2007).
- [9] F. Butler *et al.* (CLEO Collaboration), Phys. Rev. D **49**, 40 (1994).
- [10] Yu.S. Surovtsev, P. Bydžovský, R. Kamiński, V.E. Lyubovitskij, and M. Nagy, Phys. Rev. D **89**, 036010 (2014).
- [11] D. Morgan and M.R. Pennington, Phys. Rev. D **48**, 1185 (1993); **48**, 5422 (1993).
- [12] K. A. Olive *et al.* (Particle Data Group), Chin. Phys. C **38**, 090001 (2014).
- [13] Yu. A. Simonov and A. I. Veselov, Phys. Rev. D **79**, 034024 (2009).
- [14] Yu. S. Surovtsev, P. Bydžovský, R. Kamiński, V.E. Lyubovitskij, and M. Nagy, J. Phys. G **41**, 025006 (2014).
- [15] Yu. S. Surovtsev, P. Bydžovský, R. Kamiński, V. E. Lyubovitskij, and M. Nagy, Phys. Rev. D **86**, 116002 (2012).
- [16] D. -Y. Chen, X. Liu, and X. -Q. Li, Eur. Phys. J. C **71**, 1808 (2011).
- [17] Yu. S. Surovtsev, P. Bydžovský, and V. E. Lyubovitskij, Phys. Rev. D **85**, 036002 (2012).
- [18] Yu. S. Surovtsev, D. Krupa and M. Nagy, Eur. Phys. J. A **15**, 409 (2002); Czech. J. Phys. **56**, 807 (2006).
- [19] Yu. S. Surovtsev, P. Bydžovský, T. Gutsche, V. E. Lyubovitskij, R. Kamiński, and M. Nagy, Nucl. Phys. B Proc. Suppl. **245**, 259 (2013).
- [20] K.J. Le Couteur, Proc. R. Soc. A **256**, 115 (1960); R. G. Newton, J. Math. Phys. (N.Y.) **2**, 188 (1961); M. Kato, Ann. Phys. (N.Y.) **31**, 130 (1965).
- [21] N. N. Achasov and G. N. Shestakov, Phys. Rev. D **49**, 5779 (1994).